Traffic 2012; **13:** 1351–1363

doi:10.1111/j.1600-0854.2012.01398.x

The Host Endocytic Pathway is Essential for *Plasmodium berghei* Late Liver Stage Development

Mafalda Lopes da Silva[1,2], Carolina Thieleke-Matos[1,2], Laura Cabrita-Santos[1,2], José S. Ramalho[1], Silène T. Wavre-Shapton[3,4], Clare E. Futter[4], Duarte C. Barral[1,*] and Miguel C. Seabra[1,2,3,*]

[1] *CEDOC, Faculdade de Ciências Médicas, FCM, Universidade Nova de Lisboa, Lisboa 1169-056, Portugal*
[2] *Instituto Gulbenkian de Ciência, Oeiras 2780-156, Portugal*
[3] *Molecular Medicine Section, National Heart and Lung Institute, Imperial College London, London SW7 2AZ, UK*
[4] *UCL Institute of Ophthalmology, University College London, London UK*

**Corresponding authors: Miguel C. Seabra, miguel.seabra@fcm.unl.pt and Duarte C. Barral, duarte.barral@fcm.unl.pt*

The obligate intracellular liver stage of the *Plasmodium* parasite represents a bottleneck in the parasite life cycle and remains a promising target for therapeutic intervention. During this stage, parasites undergo dramatic morphological changes and achieve one of the fastest replication rates among eukaryotic species. Nevertheless, relatively little is known about the parasite interactions with the host hepatocyte. Using immunofluorescence, live cell imaging and electron microscopy, we show that *Plasmodium berghei* parasites are surrounded by vesicles from the host late endocytic pathway. We found that these vesicles are acidic and contain the membrane markers Rab7a, CD63 and LAMP1. When host cell vesicle acidification was disrupted using ammonium chloride or Concanamycin A during the late liver stage of infection, parasite survival was not affected, but schizont size was significantly decreased. Furthermore, when the host cell endocytic pathway was loaded with BSA-gold, gold particles were found within the parasite cytoplasm, showing the transport of material from the host endocytic pathway toward the parasite interior. These observations reveal a novel *Plasmodium*–host interaction and suggest that vesicles from the host endolysosomal pathway could represent an important source of nutrients exploited by the fast-growing late liver stage parasites.

Key words: endocytic pathway, late endosome, liver stage infection, lysosome, malaria, *Plasmodium berghei*

Received 26 January 2012, revised and accepted for publication 6 July 2012, uncorrected manuscript published online 10 July 2012, published online 3 August 2012

Within its mammalian host, malaria parasites (*Plasmodium* spp.) undergo two asexual replication cycles, first within hepatocytes and later within red blood cells. The invasion of hepatocytes by malaria sporozoites is characterized by the formation of a Parasitophorous Vacuole Membrane (PVM), a process involving partial invagination of the host cell plasma membrane (1), although the molecular players involved in PVM formation and maintenance remain largely unknown. Once this specialized intracellular niche is established, parasite replication and growth may commence. Dramatic morphological as well as gene expression modifications (2–4) occur at this stage and the parasites achieve one of the highest replication rates known within eukaryotic species (5).

The *Plasmodium* life cycle has been extensively characterized, but relatively little is known about the parasite interactions with the host hepatocyte. The fast multiplication rate of *Plasmodium* parasites in the liver imposes a high demand of nutrients for organelle synthesis and for this reason hepatocytes represent a favorable environment within the mammalian host. Being an obligate intracellular pathogen during this part of the life cycle also implies that all acquired nutrients must primarily come from the host cell. Intracellular pathogens have evolved different strategies in order to manipulate and divert host nutrients while evading recognition by the immune system. Key to an intracellular lifestyle is the ability to interact with the host endomembrane system and avoid pathogen degradation and elimination via fusion with lysosomes. Intracellular pathogens have evolved a variety of mechanisms to achieve this, for example, by blocking fusion with the lysosomes, as is the case with *Salmonella*, *Mycobacterium* and *Legionella* species (6–8).

Central to the interaction between parasites and the host is the PVM, a deeply convoluted membrane extending into the host cell cytoplasm and acting as a barrier between the parasite and the host. The permeability of the vacuole membrane has been shown to be actively modified to allow the passive diffusion of small molecules (<855 Da) from the host cytosol into the vacuole space through open channels (9). It was also shown by Strum et al. that the parasite membrane contains calcium-activated channels which allow for the passage of molecules from the host to the parasite cytoplasm (4).

In terms of host organelles, *Plasmodium berghei* liver stage parasites have been shown to associate with the host endoplasmic reticulum at 24 h post-infection (9,10), although the mechanism and role of this interaction remains to be elucidated. Recently, a close association between the PVM and the host mitochondria was suggested, a process thought to be important in the scavenging of lipoic acid by parasites (11). In this study, we establish that *P. berghei* parasites and the host endocytic pathway interact, and show that these interactions are

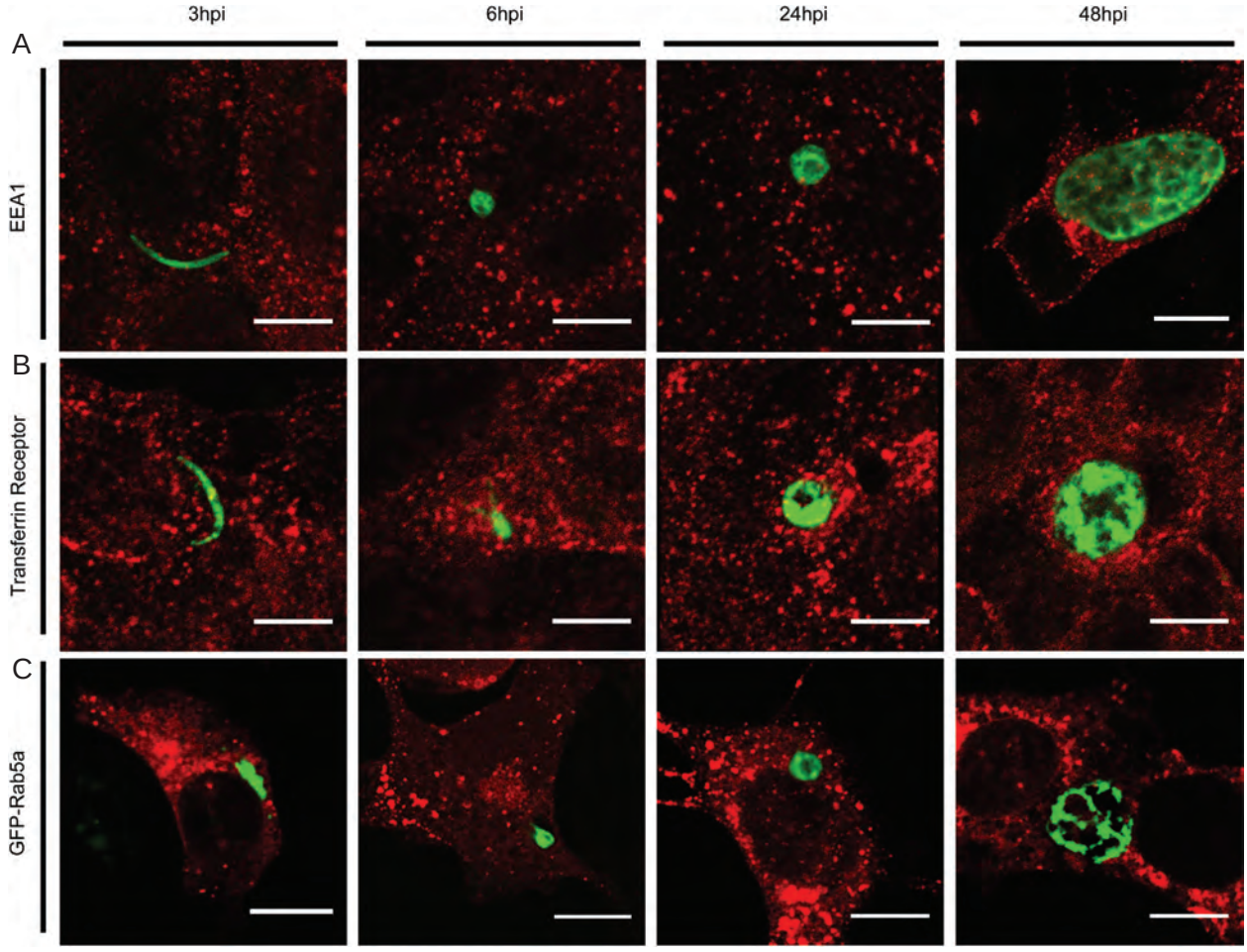

Figure 1: ***Plasmodium berghei*** **liver parasites do not interact with compartments of the host early endocytic pathway.** Hepa1-6 cells where infected with GFP-*P. berghei* sporozoites and infection was stopped at various times post-infection. A) Cells were stained with anti-Early Endosome Antigen 1 (EEA1) (red) and 2E6 (green) antibodies. B) Cells were stained with anti-TfR (red) and anti-GFP (green) antibodies. C) Hepa1-6 cells were transduced with GFP-Rab5a (red) prior to infection with *P. berghei* sporozoites, fixed at the time-points indicated and subsequently stained with 2E6 antibody (green). Hpi, hours post-infection. Scale bars: 10 μm.

crucial for parasite growth during the late stages of liver infection.

Results

Plasmodium berghei *liver parasites are surrounded by vesicles from the host late endocytic pathway*

To identify any possible cellular interactions between host hepatocyte organelles and *P. berghei* parasites, proteins known to be present on different organelles of the mammalian endomembrane system were analyzed at various stages during liver infection, using indirect immunofluorescence. Hepa1-6 cells were infected with freshly dissected green fluorescent protein (GFP)-expressing *P. berghei* sporozoites, fixed at various times post-infection and stained for early and recycling endosomes, using the widely used protein markers early endosome antigen 1 (EEA1) and transferrin receptor (TfR), respectively (Figure 1A and B and separate channels in Figure S1A). To visualize Rab5a-positive vesicles, Hepa1-6 cells were transduced with GFP-Rab5a prior to infection (Figure 1C). The parasite cytoplasm was stained either using 2E6, which recognizes *P. berghei* cytoplasmic heat-shock protein 70 or anti-GFP antibodies. We found that there was no specific reorganization or accumulation of either early or recycling endosomes in *P. berghei*-infected cells, in the time-points studied. Conversely, when similar experiments were performed using membrane markers of late endosomes and lysosomes, such as Lysosome-Associated Membrane Protein 1 (LAMP1) (Figure 2A), GFP-Rab7a (Figure 2B and separate channels in Figure S1B) and CD63 (LAMP3) (Figure 2C), a distinctive accumulation of labeled structures was seen surrounding *P. berghei* parasites. The same accumulation pattern of LAMP1-stained structures was observed in infected murine primary hepatocytes, suggesting that this phenomenon is physiologically relevant (Figure S1C).

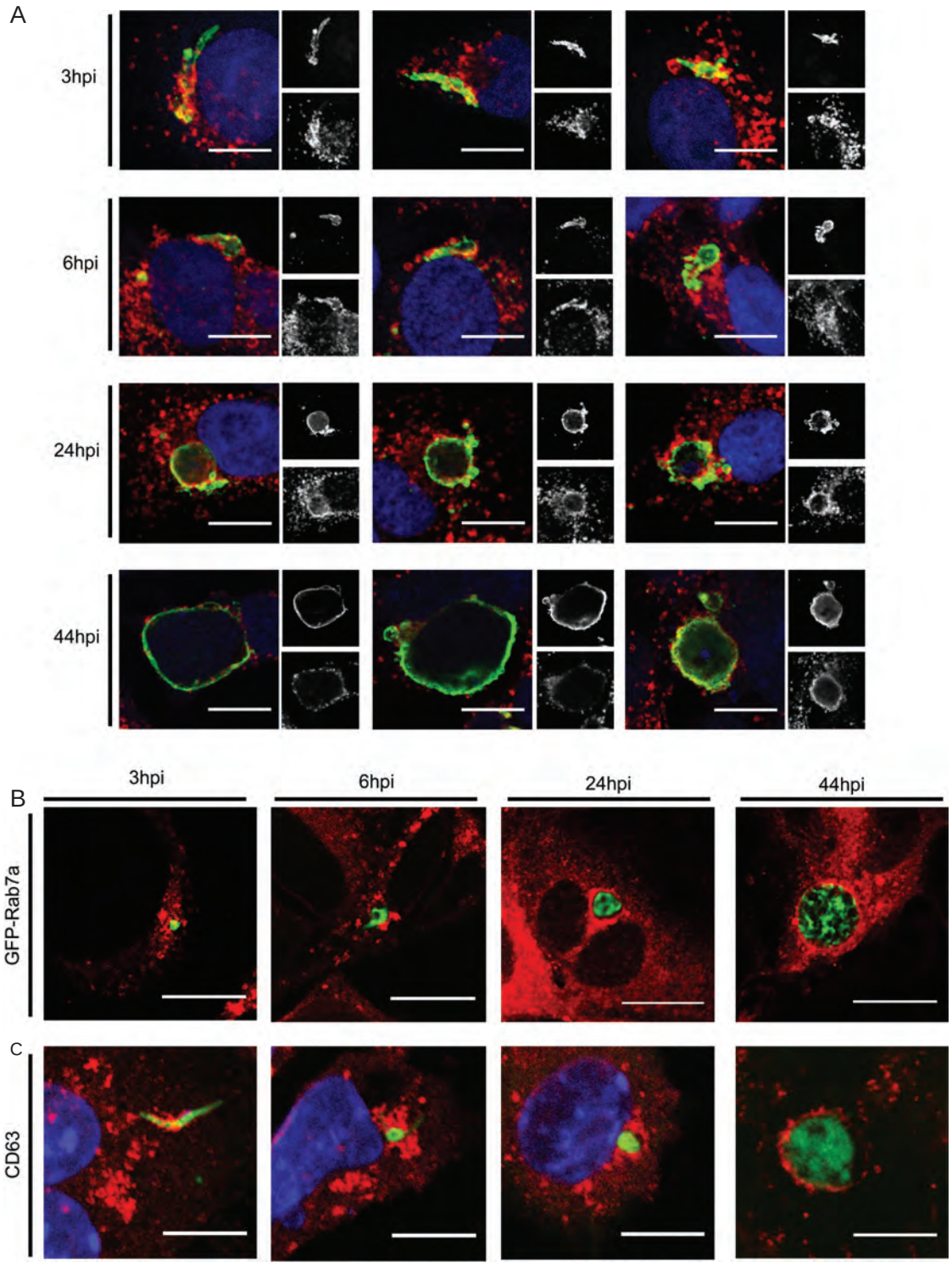

Figure 2: *Plasmodium berghei* liver parasites are surrounded by vesicles from the host late endolysosomal pathway. A) Hepa1-6 cells where infected with *P. berghei* sporozoites and infection was stopped at various times post-infection. Cells were stained with anti-LAMP1 antibody (red) and the anti-UIS4 (PVM marker) antibody (green). Three representative images for each time-point are shown. Nuclei were stained with DAPI. Insets show the individual stainings (top, anti-UIS4; bottom, anti-LAMP1). B) Hepa1-6 cells were transduced with GFP-Rab7a (red) prior to infection with *P. berghei* sporozoites, fixed at the time-points indicated and subsequently stained with 2E6 antibody (green). C) Samples were stained with anti-CD63 (red) and anti-GFP (green) antibodies. Hpi, hours post-infection. Scale bars: 10 μm.

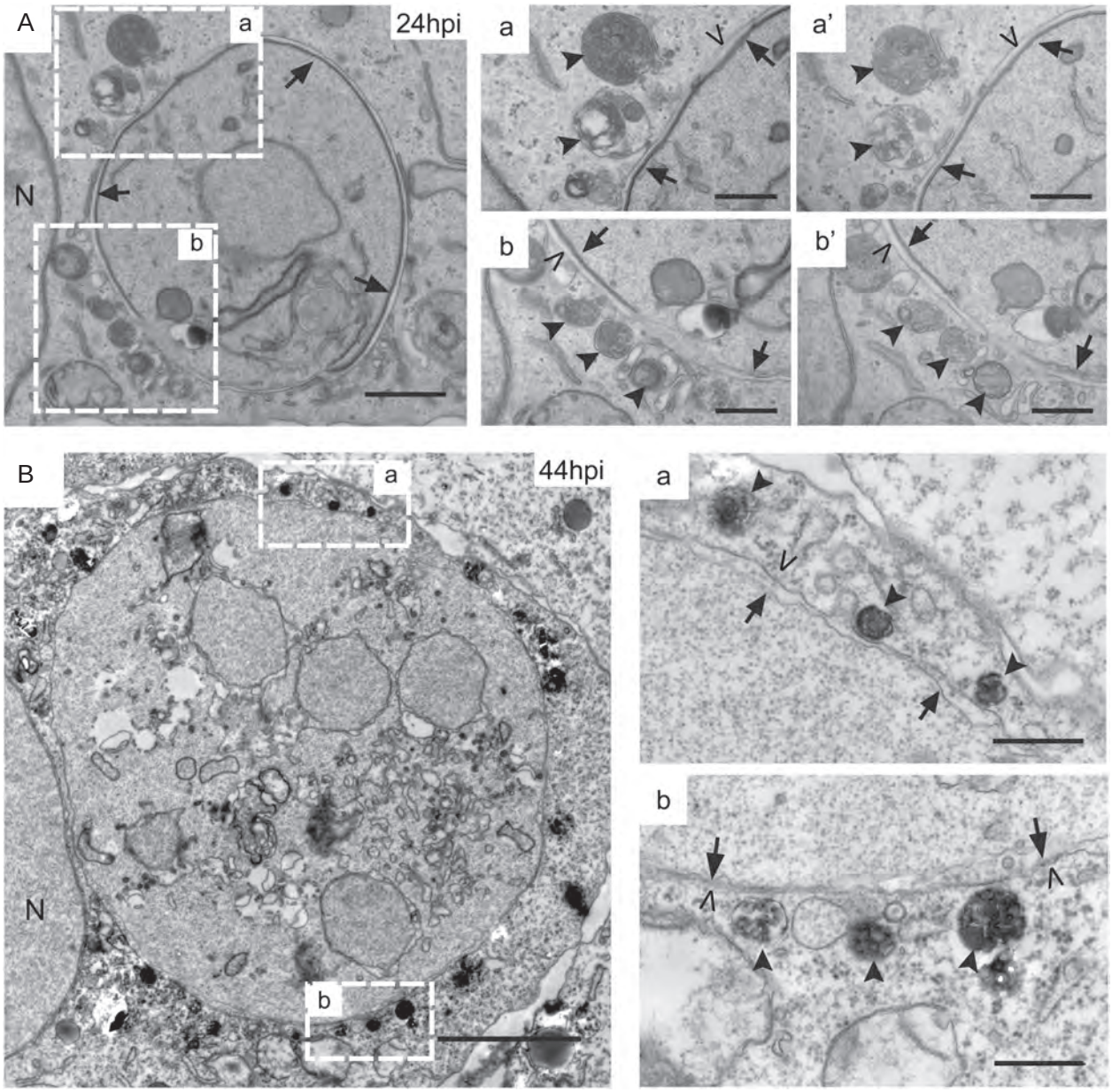

Figure 3: *Plasmodium berghei* parasites are surrounded by vesicles originating from the host endocytic pathway. A) Hepa1-6 cells were infected with *P. berghei* sporozoites and samples were prepared for TEM analysis 24 h post-infection. Electron micrograph showing a parasite cross section with the parasite membrane (arrows), the PVM (arrowheads) and various host vacuoles surrounding the PVM (filled arrowheads). Insets show two serial sections of the areas highlighted. N, host nucleus. Scale bars: 1 μm and 500 nm in insets. B) Electron micrograph of a *P. berghei* parasite 44 h post-infection where cells were incubated with HRP for 12 h prior to fixation, followed by DAB reaction. HRP appears in black. The parasite membrane (arrows), the PVM (arrowheads) and various HRP vacuoles surrounding the PVM (filled arrowheads) are indicated. Insets show two magnified images of the areas highlighted. Scale bar: 3 μm and 500 nm in insets. Hpi, hours post-infection.

To further characterize these structures, samples were prepared for Transmission Electron Microscopy (TEM). At 24 h post-infection, the PVM of *P. berghei* parasites within Hepa1-6 cells was surrounded by various types of host organelles, resembling multivesicular bodies and lysosome-like structures containing internal membranes and vesicles of various sizes (Figure 3A). To determine whether these structures were derived from the endolysosomal pathway, cells were infected and incubated with horseradish peroxidase (HRP) for 12 h prior to fixation. Using this approach, HRP is taken up by cells through endocytosis, and traffics through the entire endocytic pathway. After fixation, a diaminobenzidine (DAB) reaction was performed, allowing the visualization of the HRP

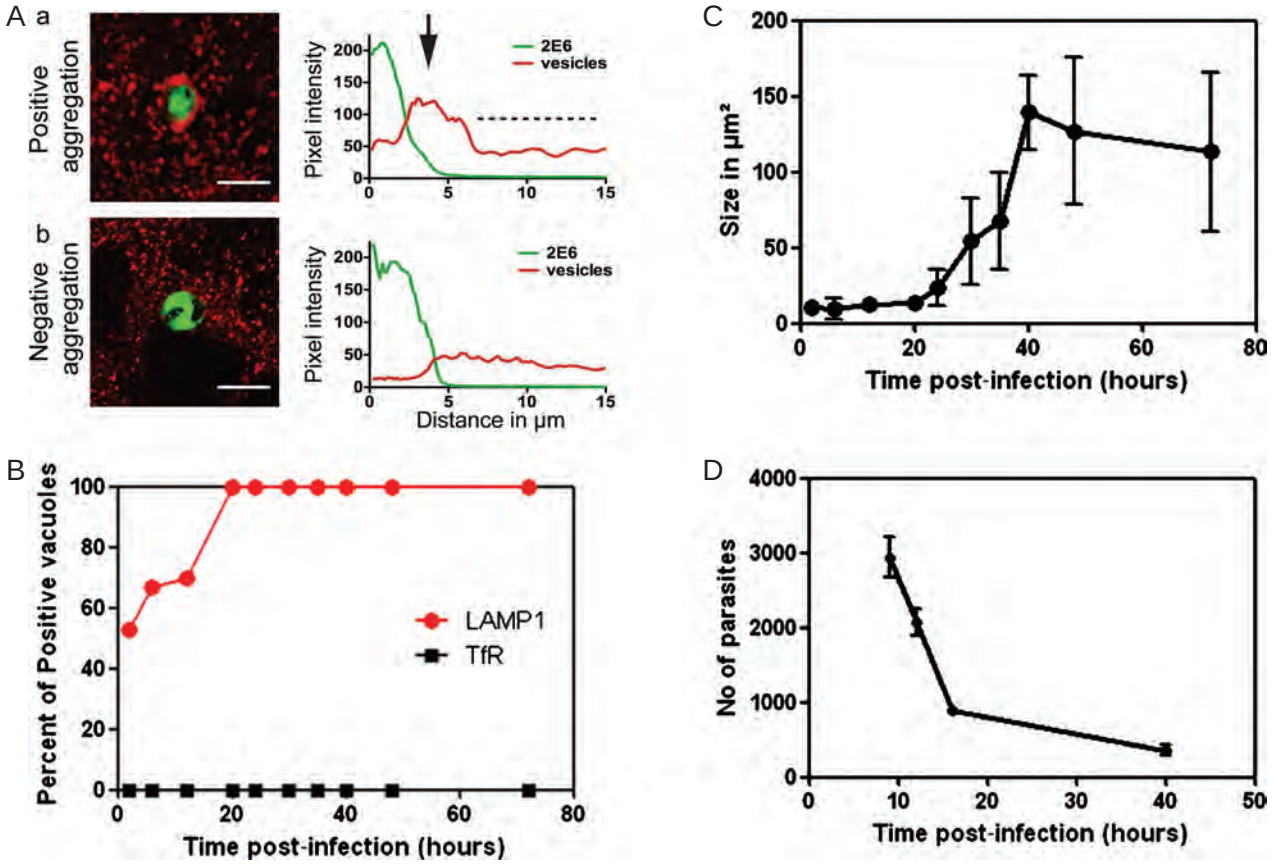

Figure 4: Kinetics of acquisition of LAMP1 and transferrin receptor-positive vesicles surrounding *Plasmodium berghei* liver parasites. A) Images of intracellular parasites where (a) positive and (b) negative vesicle aggregation can be observed. Radial intensity plots for each parasite showing cytoplasmic levels (dashed lines) and the fluorescence intensity peak in the case of aggregation around the parasite (arrow). Parasites are shown in green and vesicles in red. Scale bar: 10 µm. B) Hepa1-6 cells were infected with *P. berghei* sporozoites, infection was stopped at the time-points indicated and processed for immunofluorescence analysis. Cells were either stained with anti-LAMP1 (red line) or anti-TfR antibody (black line). At least 50 internalized parasites per time-point were analyzed and scored for either positive or negative aggregation of stained vesicles. C) In the same experiment as in (B), mean parasite size was calculated for each time-point by measuring the area occupied by parasites in μm^2 using ImageJ software. D) Hepa1-6 cells were infected with 4×10^4 sporozoites and infection was stopped at the time-points indicated. Cells were stained with 2E6 and anti-UIS4 antibodies, to distinguish intracellular parasites. The total number of parasites in each coverslip was counted. Shown are mean values of triplicate samples for the time-points indicated.

throughout the endolysosomal pathway. Multiple HRP-containing vesicles were seen within 5–20 nm of the PVM (Figure 3B), indicating that the structures that aggregate around the parasite PVM originate from the host endolysosomal pathway.

To quantify the host vesicle aggregation, at least 50 parasites within Hepa1-6 cells at various times post-infection, were stained and scored for either 'positive' or 'negative' aggregation (see *Materials and Methods* and Figure 4A). During the early hours of infection (between 3 and 12 h post-infection), 50 to 70% of the parasites analyzed had a significant accumulation of LAMP1-stained vesicles and this number increased to 100% by 20 h post-infection (Figure 4B, red line). As expected, when the same quantification was done for TfR-positive vesicles, no accumulation was observed throughout the entire duration of the liver infection (Figure 4B, black line). To rule out that vesicle aggregation was an artifact of the parasite occupying most of the host cytoplasm during growth, the average size of parasites, calculated by measuring the area of parasite cytoplasm, was determined (Figure 4C). We observed that LAMP1-positive vesicle aggregation occurs in 100% of parasites before any significant parasite size increase occurs (after 20 h post-infection), suggesting that LAMP1-vesicle aggregation is not due to the parasite occupying a large area of the host cell cytoplasm.

As not all parasites that invade hepatocytes are able to survive and reach the later stages of liver infection (Figure 4D), we initially hypothesized that the vesicles surrounding *Plasmodium* parasites were part of the cell defense mechanisms, in an attempt to degrade and eliminate growing parasites. This is typically achieved

by fusion of highly acidic degradative lysosomes with the vacuole membrane of intracellular pathogens, allowing for the active proteases within the acidic lysosome environment to be discharged into the vacuole space (12). As a significant number of parasites are able to survive and develop to produce viable merozoites, we concluded that some parasites are able to subvert this host cellular defense mechanism in order to establish a successful infection. Thus, we proceeded to analyze the relative acidity of the structures surrounding parasites and their possible role during *P. berghei* infection.

Plasmodium berghei *parasites are surrounded by acidic vesicles*

Live cell imaging using GFP-*P. berghei*-infected cells was performed to investigate the relative acidity of the vesicles surrounding parasites throughout the infection cycle. LysoTracker®Red is a dye that is freely permeable to cell membranes and selectively accumulates in cellular compartments with a low internal pH, such as lysosomes. Hepa1-6 cells were infected with GFP-*P. berghei* sporozoites and infection was allowed to proceed. LysoTracker®Red was added to the cells 5 min prior to visualization and representative images of selected time-points are shown in Figure 5. As expected, LysoTracker®Red-positive vesicles clustered around *P. berghei* parasites throughout hepatocyte infection in a punctate pattern (Figure 5A). This is markedly different from the pattern observed when these cells were fed latex beads, where fusion with acidic lysosomes occurs and LysoTracker®Red becomes evenly distributed throughout the perimeter of the bead (Figure S2A). Time-lapse microscopy allows the visualization of the movement and dynamics of vesicles, a dimension that is lost in fixed cells. Interestingly, using this technique we observed that some vesicles stabilized on the parasite vicinity and stopped movement altogether (Figure 5B, dashed square), while others were seen in close contact with the parasite, but then moved away (Figure 5B, arrow, and Movie S1). Notably, the area occupied by the parasite was always negative for LysoTracker®Red.

To further analyze the luminal pH of these vesicles, we used pHrodo™dextran, a pH-sensitive dye that is non-fluorescent in neutral pH, fluoresces bright red as the pH decreases and enters the cell through endocytosis. Hepa1-6 cells were incubated with this dye for 12–16 h followed by washing and chasing in growth medium for 2–3 h. Using this protocol, pHrodo™dextran accumulates in late endosomes/lysosomes. GFP-*P. berghei* parasites in cells incubated with pHrodo™dextran showed acidic vesicles in close proximity to the PVM, in a punctate staining pattern, at all time-points tested (Figure 6). Conversely, when the same cells were fed latex beads, we observed a continuous fluorescent rim, consistent with internal vacuole acidification (Figure S2B). As seen with LysoTracker®Red, pHrodo™dextran did not stain the parasitophorous vacuole area, suggesting that the internal vacuole space does not become acidic.

Interfering with host acidic vesicles disrupts parasite growth

To investigate the role of the vesicles that aggregate around *P. berghei* vacuoles during liver infection, we proceeded to interfere with their biogenesis and function. A key aspect of lysosomes is their low internal pH, which is instrumental for their function (13). Lysosome function can be disrupted by dissipating the pH gradient across lysosomes, using a weak base such as ammonium chloride (NH_4Cl) (14), or by inhibiting the v-ATPase pump using drugs such as Concanamycin A (15,16). Both methods were used in the context of malaria liver cell infection.

To confirm that these treatments were affecting Hepa1-6 as expected, cells treated with 25 mM NH_4Cl or 0.1 nM of Concanamycin A for 24 h were fixed and stained with anti-LAMP1. Late endosomes/lysosomes were compromised in their morphology after NH_4Cl or Concanamycin A treatment as previously described (16,17) (Figure 7A). Consistently, when cells were incubated with pHrodo™dextran and treated with NH_4Cl or Concanamycin A, the fluorescence intensity of the pHrodo™dextran staining decreased significantly (Figure 7A). Quantification of the fluorescence intensity of these pHrodo™dextran-stained vesicles showed that the ones with a high intensity value (very acidic) disappeared and only vesicles with a low fluorescence intensity (less acidic) remained in the treated cells (Figure 7B–D). No significant cell death was observed even after prolonged treatments (24 h) (data not shown). Hepa1-6 cells were infected with freshly dissected *P. berghei* parasites and infection proceeded for 16 h, a time when parasite replication and growth is initiated. Cells were then incubated with either growth medium (control), 25 mM NH_4Cl or 0.1 nM Concanamycin A and fixed for immunofluorescence staining at 40 h post-infection. Total number of parasites per coverslip and schizont size were quantified. Although, the total number of parasites at 40 h post-infection was not altered (Figure 7E) suggesting that these treatments did not affect parasite survival, mean schizont size was significantly decreased in treated cells when compared to control cells (mean size of 96.19 μm^2 in control versus 30.71 μm^2 in NH_4Cl and 53.65 μm^2 in Concanamycin A-treated cells, $p = 0.0001$; Figure 7F and G). These results point toward a possible role of host acidic vesicles in parasite growth rather than in parasite killing, during the late stages of liver infection.

Collectively, our data suggest that vesicles from the host endolysosomal pathway play a role in *P. berghei* late liver parasite growth, possibly acting as a source of nutrients.

Interestingly, electron micrographs of parasites at 24 h post-infection revealed various small vesicles with sizes ranging from 30 to 150 nm between the PVM and the parasite membrane (Figure 8). These were very similar to the nearby host vesicles and their content (Figure 8Ca). Although it cannot be excluded that these small vesicles

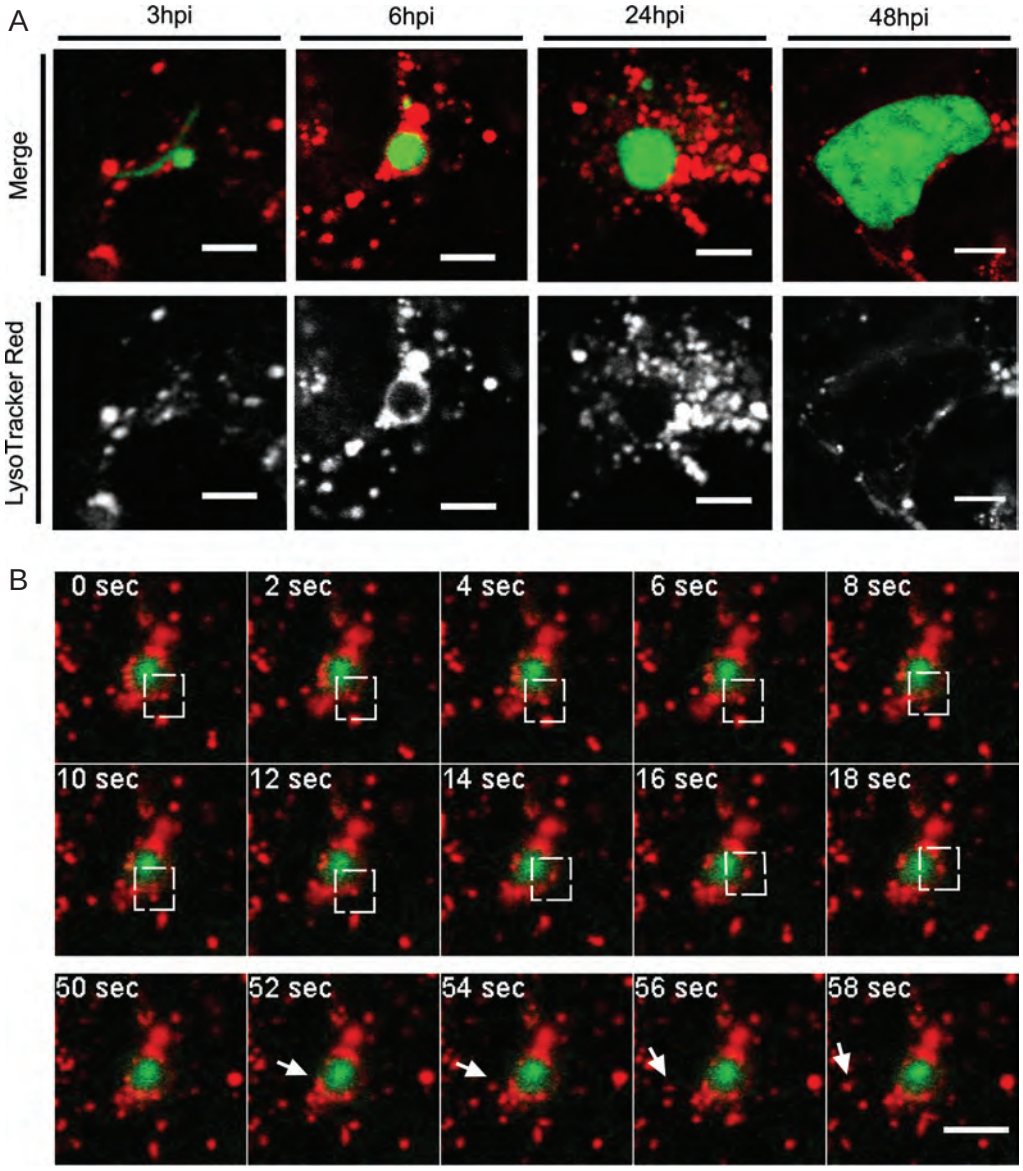

Figure 5: LysoTracker®Red acidic vesicles aggregate around *P. berghei* liver parasites. A) Hepa1-6 cells were infected with GFP-*P. berghei* sporozoites and infection was allowed to proceed. Prior to visualization at the indicated time-points, LysoTracker®Red was added to the cells. Parasites are shown in green and LysoTracker®Red-stained vesicles are shown in red. Scale bar: 5 μm. B) Time-lapse images showing the dynamic movement of LysoTracker®Red positive vesicles around a *P. berghei* parasite at 16 h post-infection. A vesicle that moves toward the parasite and stabilizes on the PVM (dashed square) and another that moves away from the PVM (arrow) are indicated. Full movie can be watched in Movie S1. Hpi, hours post-infection. Scale bar: 5 μm.

originated from the parasite exocytic pathway, we tested whether some of these vesicles could be originating from the host endolysosomal pathway. When cells were incubated with HRP for 12 h prior to fixation and DAB histochemistry, it was possible to find DAB reaction product within parasite vacuoles, at 44 h post-infection (Figure 9A). Although HRP is a very sensitive probe, the DAB reaction product can disperse when not confined within a membranous organelle and become difficult to distinguish from the surrounding electron dense cytoplasm. Therefore, cells were incubated with another fluid phase marker which is endocytosed similarly to HRP, namely BSA-gold, for 16 h prior to fixation, allowing the uptake and distribution of gold particles throughout the host endocytic pathway. We observed gold particles in four distinct locations: in vesicles from the host endolysosomal pathway (Figure 9Ba); in vesicles within the parasitophorous vacuole (Figure 9Ba); in vesicles inside the parasite (Figure 9Bb); and in the parasite cytoplasm (Figure 9Bc). In host cells, as expected, gold particles were only observed within membrane-bound vesicles from the host endolysosomal pathway. Thus, the presence of gold inside

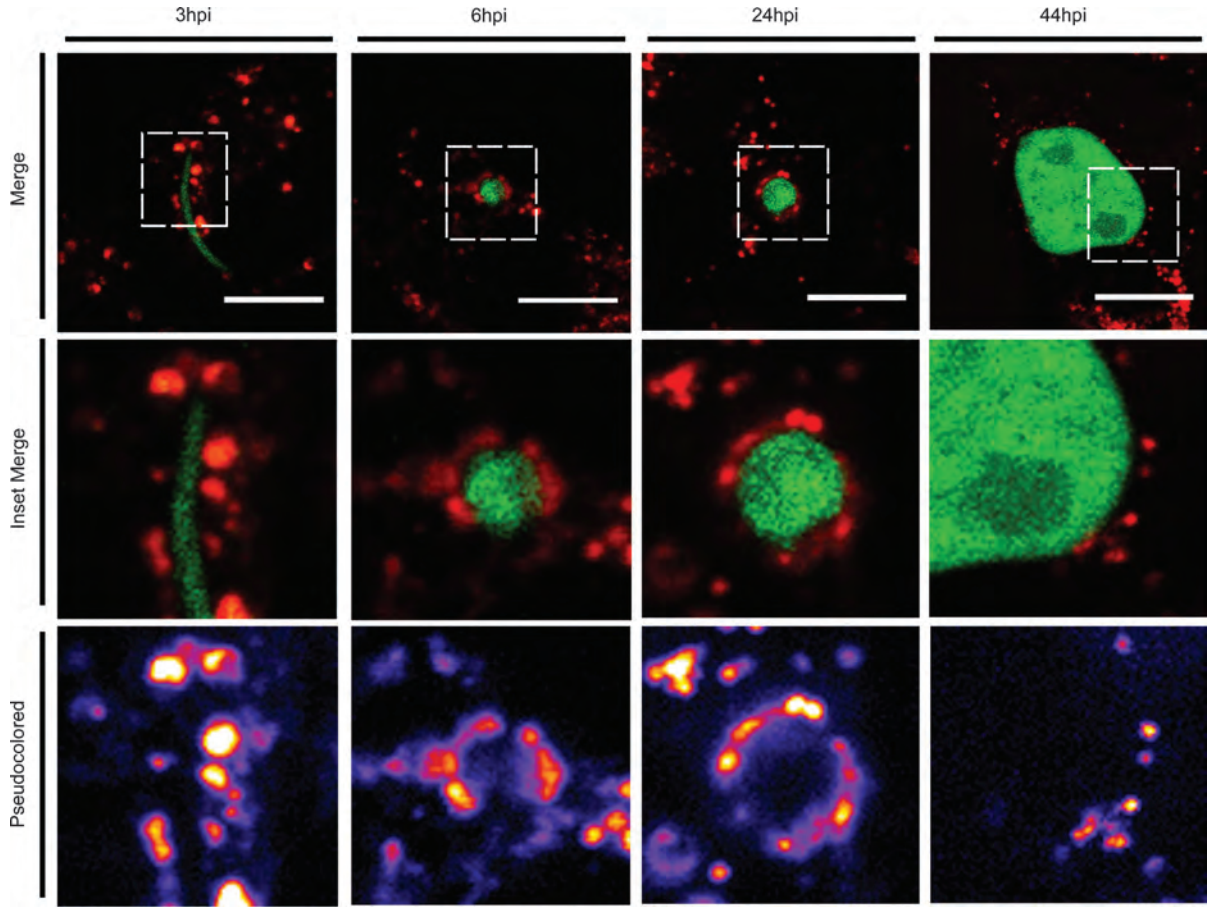

Figure 6: *Plasmodium berghei* liver parasites are surrounded by acidic vesicles but maintain a neutral vacuole pH. For visualization of parasites at 3 and 6 h post-infection, Hepa1-6 cells were incubated with pHrodo™dextran (red and pseudocolored) overnight prior to washing and infection with GFP-*P. berghei* (green). For visualization of parasites at 24 and 44 h post-infection, Hepa1-6 cells were infected with GFP-*P. berghei* parasites and once parasites had invaded, cells were incubated with pHrodo™dextran. pHrodo™dextran vesicles are either shown in red or have been pseudocolored so that less intense vesicles (more neutral) are purple and more acidic vesicles are pink/white. Hpi, hours post-infection. Scale bars: 10 μm.

parasites strongly suggests an influx of cargo originating from the host endocytic pathway, which is able to cross both the PVM membrane and the parasite membrane.

We then tested the effect of disrupting late endocytic vesicle fusion and function on the traffic of endocytic cargo into the parasite vacuole, using NH_4Cl, as this was the treatment with the most striking effect on parasite growth. For this, infected cells were incubated with control growth medium or 25 mM NH_4Cl after 16 h of infection, and BSA-gold was added 16 h prior to fixation at 44 h post-infection. Samples were prepared for conventional TEM and random sections were analyzed for gold content inside the parasite vacuole (Figure 9C). As predicted, only 10% of the parasites analyzed had at least one gold particle (in a random section) in NH_4Cl-treated cells, compared with 40% of parasites in the control sample. The number of gold particles per parasite was also dramatically decreased, with an almost 40-fold difference in the number of gold particles per parasite in control versus NH_4Cl-treated cells. These results suggest that delivery of endocytic contents to the parasitic vacuole and to the parasite is severely inhibited by NH_4Cl treatment.

Interestingly, various host vesicles containing gold particles were observed in very close proximity to the PVM (<20 nm), suggesting the formation of membrane contacts between the two structures (Figure 9D). These contacts were observed in both control and NH_4Cl-treated cells, indicating that NH_4Cl treatment did not prevent their formation, but probably inhibited subsequent fusion with the PVM.

Discussion

Here, we present for the first time evidence that *P. berghei* liver parasites are surrounded by host late endosomes and lysosomes while no clear aggregation of early and recycling endosomes was observed. Furthermore, we

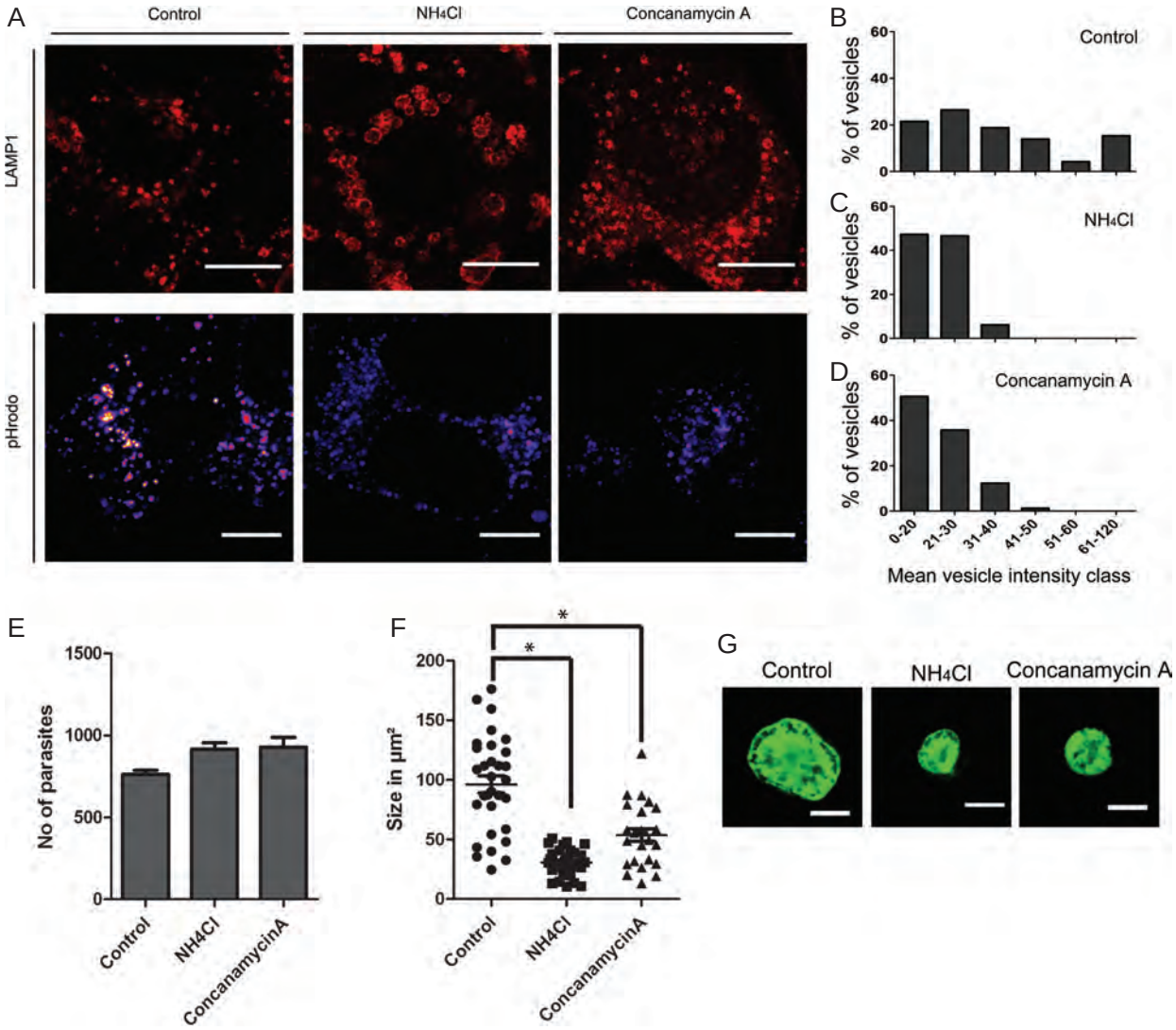

Figure 7: Disruption of host vesicle acidification impairs *P. berghei* liver growth. A) Hepa1-6 cells were incubated with growth medium (control), 25 mM NH_4Cl or 0.1 nM Concanamycin A for 24 h and either prepared for immunofluorescence and stained with anti-LAMP1 antibody (top panel) or incubated with pHrodo™dextran (bottom panel). pHrodo™dextran images are pseudocolored so that less intense vesicles (more neutral) are purple and more intense vesicles (more acidic) are shown in pink and white. Scale bar: 10 µm. B) Quantification of the mean intensity of pHrodo™dextran-stained vesicles in control cells. C) Quantification of the mean intensity of pHrodo™dextran-stained vesicles in NH_4Cl-treated cells. D) Quantification of the mean intensity of pHrodo™dextran-stained vesicles in Concanamycin A-treated cells. E) Hepa1-6 cells were infected with *P. berghei* sporozoites and infection was left to proceed for 16 h before the addition of growth medium (control), 25 mM NH_4Cl or 0.1 nM Concanamycin A. Samples were fixed at 40 h post-infection and stained with 2E6 antibody. The total number of parasites at 40 h post-infection in triplicate wells was quantified. F) In the same experiment as in E, schizont size was quantified by measuring the area occupied by schizonts in μm^2. *p-Value = 0.0001. G) Representative images of parasites at 40 h post-infection in control, NH_4Cl and Concanamycin A-treated cells stained with 2E6 antibody. Scale bars: 5 µm.

show that parasites are surrounded by highly acidic vesicles and that disruption of host cell vesicle acidification results in delayed parasite growth. Taken together, these observations reveal a novel *Plasmodium*–host cellular interaction, where host vesicles from the endolysosomal pathway could be important for schizont development.

The cellular and molecular interactions that occur between the malaria parasite and the host liver cell remain largely unknown. In this study, we show that *Plasmodium* parasites are surrounded by host late endosomes/lysosomes, as determined by the presence of the markers LAMP1, Rab7a, CD63, LysoTracker®Red, pHrodo™Dextran and TEM vesicle morphology. Interestingly, a similar observation has been made for the related apicomplexa *Toxoplasma gondii* where parasites in VERO cells were surrounded by LysoTracker®Red and LAMP1-containing structures (18).

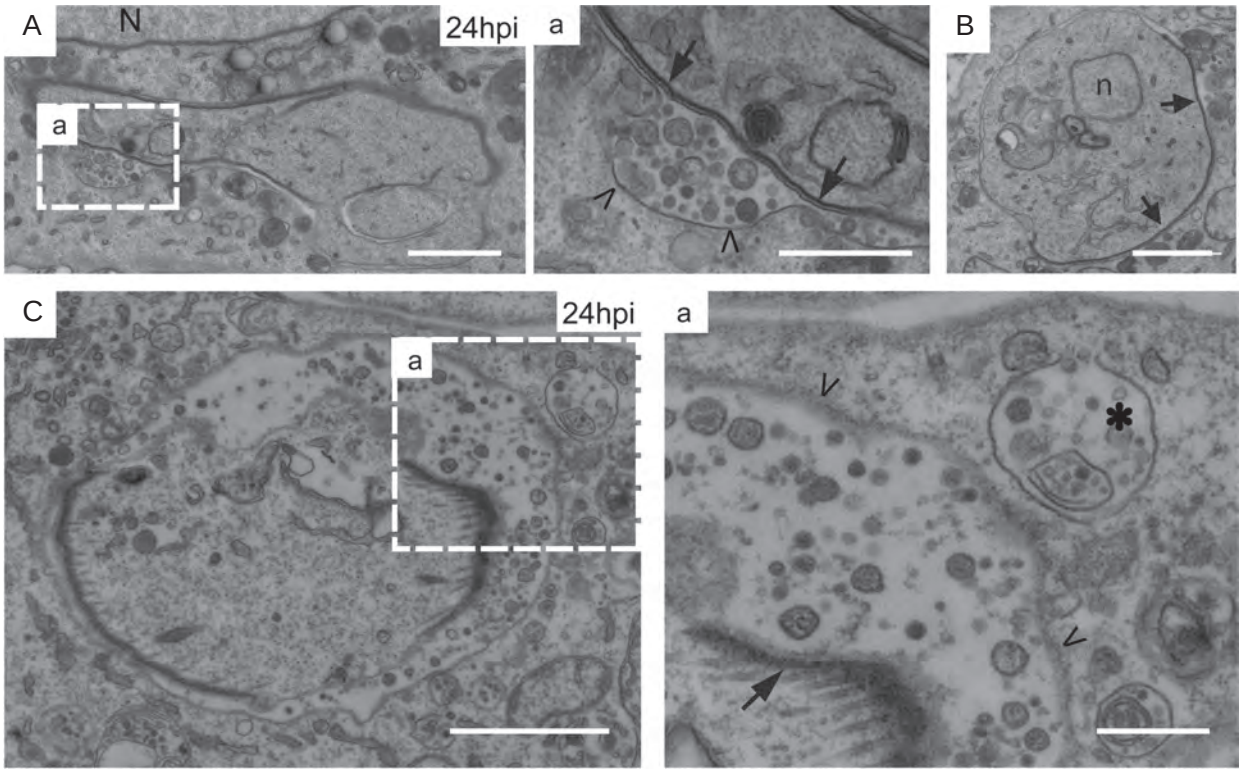

Figure 8: *Plasmodium* vacuoles contain material with similar morphology to that found in host vesicles. A) Hepa1-6 cells were infected with *P. berghei* sporozoites and samples were prepared for TEM analysis at 24 h post-infection. Electron micrograph showing a parasite cross section where the vacuolar space is seen. Inset shows the area highlighted, where multiple small vesicles are visible within the vacuole space. Parasite membrane (arrows) and the PVM (arrowheads) are indicated. N, host nucleus. Scale bars: 1 μm and 500 nm in inset. B) In order to confirm the integrity of the parasite shown in (A), a different serial section of the same parasite is shown. It is possible to see the integrity of the parasite nucleus (n) as well as parts of the inner membrane complex (arrows). Scale bar: 1 μm. C) Another example of a TEM image of a *P. berghei* parasite at 24 h post-infection where the parasitophorous vacuole space can be seen full of small vesicles which are between 30 and 150 nm in diameter and resemble the contents of nearby host structures. Inset shows area highlighted. Parasite membrane with its inner membrane complex (arrows), the PVM (arrowheads) and host vacuoles (*) are indicated. Scale bar: 1 μm and 300 nm in inset. Hpi, hours post-infection.

As we showed that lysosomes surround the parasite, we decided to investigate their role during *Plasmodium* development. Two alternative hypotheses are that these vesicles act as a host defense mechanism, or alternatively, that they could somehow be used by the parasite for its own benefit, possibly as a rich source of nutrients. When we disrupted host vesicle acidification during the replicative stage of parasite development, using NH_4Cl or Concanamycin A, which compromises trafficking and fusion, we observed no effect on parasite infection rates. This suggests that the lysosomes surrounding parasite vacuoles are not responsible for parasite clearance during late-liver infection. Furthermore, the interaction of viable parasites with the host endolysosomal pathway does not appear to involve fusion between highly acidic vesicles, such as mature lysosomes, as our data indicate that there is no acidification of the parasitophorous vacuole. Indeed, it would be expected that highly acidic vesicle contents discharged into the parasitophorous vacuole space would severely compromise parasite viability, which clearly does not happen, at least to a significant population of parasites that is able to withstand liver stage development and produce viable merozoites. We speculate that fusion with highly acidic vesicles with the PVM could be important in the clearance of those parasites that do not withstand the entire liver stage, although we could not measure the acidity of dying parasite vacuoles as they are quickly eliminated in culture conditions.

Surprisingly, when host acidic vesicles were disrupted during the growth phase of parasite development, parasites were significantly smaller at 40 h post-infection compared to control cells, pointing toward the hypothesis that late endocytic vesicles could be an important nutrient source for *Plasmodium* late liver stage development. We speculate that compartments of the host endolysosomal pathway fuse with the PVM but, in order to avoid degradation following the discharge of the highly acidic content of mature lysosomes, parasites need to be able to control precisely these fusion events. This selective fusion process could avoid the discharge of the highly degradative mature lysosome contents into the parasite vacuole

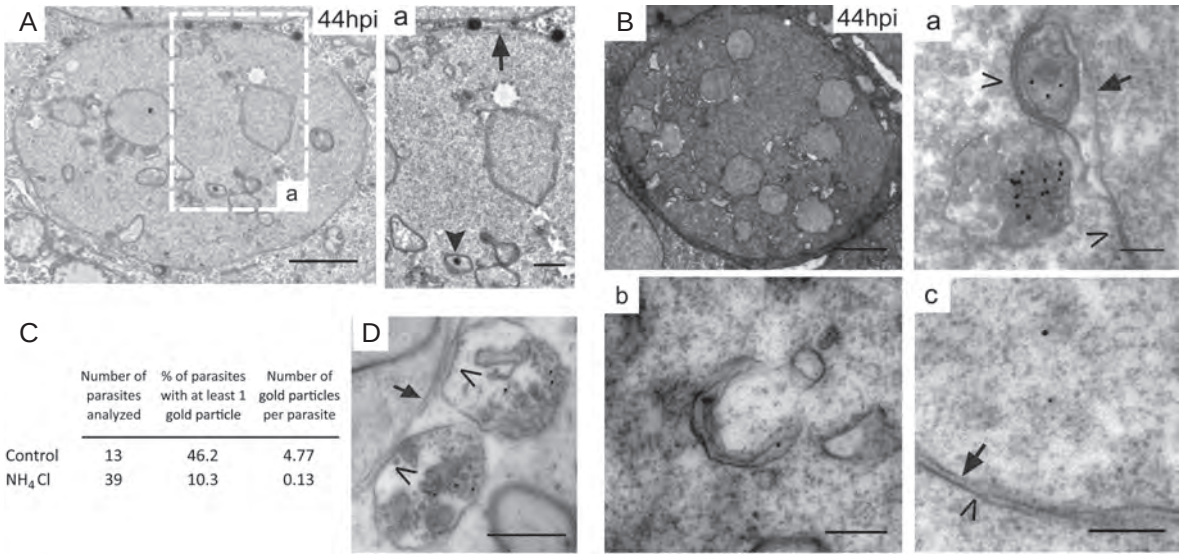

	Number of parasites analyzed	% of parasites with at least 1 gold particle	Number of gold particles per parasite
Control	13	46.2	4.77
NH_4Cl	39	10.3	0.13

Figure 9: Material originating from the host endocytic pathway is able to traverse the *Plasmodium* parasitophorous vacuole membrane and the parasite membrane. A) Electron micrograph of a *P. berghei* parasite at 44 h post-infection where cells were incubated with HRP for 12 h prior to fixation, followed by DAB reaction. HRP appears in black. Insets show a higher magnification of the area highlighted. HRP vacuoles are found around the PVM (arrow) but also inside the parasite (filled arrowhead in inset). Scale bar: 3 and 1 μm in inset. B) TEM image of a *P. berghei* parasite at 44 h post-infection where cells were incubated with 10 nm BSA-gold for 16 h prior to fixation. A cell containing a parasite was identified and then serial sections were examined to determine the gold distribution. Gold particles were observed in four distinct locations: (a) in host vesicles from the host endocytic pathway; (b) in vesicles within the parasitophorous vacuole space; (c) in vesicles inside the parasite membrane and (d) in the parasite cytoplasm. Parasite membrane (arrows) and the PVM (arrowheads) are indicated. Scale bar: 3 μm and 200 nm in (a), (b) and (c). C) Quantification of gold particles inside parasite vacuoles in control and NH_4Cl-treated cells. The number of gold particles found in random sections was quantified for each parasite where BSA-gold was fed to infected cells 16 h prior to fixation. D) Example of membrane contacts (arrowhead) between the limiting membrane of vesicles from the host endolysosomal pathway and the PVM (arrow) in a NH_4Cl-treated cell. Scale bar: 500 nm.

space, by only allowing PVM fusion with the more mildly acidic compartments of the endolysosomal pathway. In addition, the parasite vacuole could have some pH buffering capacity, allowing for some acidic content discharge without a significant decrease in vacuole pH. The presence of endocytosed BSA-gold in the parasite cytoplasm implies that following selective discharge of endocytic contents into the parasite vacuole space, this content can then be taken up by the parasite. The dramatic decrease in the amount of BSA-gold particles found inside parasite vacuoles in NH_4Cl-treated cells (Figure 9C) shows that fusion between the host endolysosome and the PVM was impaired by this treatment, further suggesting a decrease in the acquisition of nutrients from the host cell for growth.

Alternatively, *Plasmodium* could have developed a delivery system such as the one described for *Toxoplasma* called H.O.S.T. (Host organelle-sequestering tubule-structures) (18). This is a unique unidirectional transport mechanism, where microtubule-based invaginations of the PVM serve as conduits for the delivery of a diverse range of components from the host endolysosomal pathway to the *Toxoplasma* vacuole. Future studies should investigate whether this mechanism is also used by intrahepatic *Plasmodium* sporozoites although similar structures were never observed in our TEM images.

In conclusion, our study provides the basis for a better understanding of the molecular players underlying parasite growth in the mammalian host during malaria liver infection, which may lead to the development of novel therapeutic approaches.

Materials and Methods

Cell lines and culture conditions

Mouse hepatoma cell line Hepa1-6 (ATTC) was generously provided by M.M.Mota (IMM, Lisbon) and cells were cultured in Dulbecco's Modified Eagle Medium (DMEM) (Gibco/Invitrogen) supplemented with 10% Fetal Calf Serum (FCS) (Gibco/Invitrogen), 100 U/mL penicillin and 100 μg/mL streptomycin (Gibco/Invitrogen). Cells were maintained in a humidified incubator at 37°C and 10% CO_2. Primary mouse hepatocytes were isolated from female C57BL/6 mice (8–10 weeks old) according to the protocol described by Gonçalves et al. (19). All mice were bred and housed at the Instituto Gulbenkian de Ciência animal house facility and animal handling was conducted in accordance with institutional animal care guidelines and committee-approved protocols.

Parasite strains, cultivation and infection

Plasmodium berghei ANKA and GFP expressing *P. berghei* ANKA (parasite line 259cl2) (20) salivary gland sporozoites were collected from infected female *Anopheles stephensi* mosquitoes. Mosquitoes were bred in the insectarium of the Instituto de Medicina Molecular, Lisbon, and were kindly provided by M.M.Mota. Mosquitoes infected with *P. berghei or*

GFP-*P. berghei* parasites were dissected between days 20 and 24 after the infectious blood meal. Mean number of sporozoites was determined using a hemocytometer. Parasites were added to confluent cells on coverslips and plates were centrifuged at 3000 rpm for 5 min at 4°C for parasites to come into contact with the cells.

Immunofluorescence microscopy sample preparation

Hepa1-6 cells (9×10^4) were seeded on coverslips on 24-well plates. At the appropriate time-points, cells were washed twice with PBS, and fixed with 4% paraformaldehyde (PFA) (Electron Microscopy Sciences) in PBS for 15 min at room temperature. Cells were washed twice in PBS and incubated for 10 min with 10 nM NH_4Cl to quench the remaining PFA. Cells were blocked and permeabilized with 1% BSA (Bovine Serum Albumin, Sigma), 0.05% saponin (Sigma) and 1% FCS (Gibco/Invitrogen) in PBS for 30 min. Cells were incubated with primary antibodies in the same solution for 1 h. After washing in PBS, cells were incubated with secondary antibodies in the same solution for 30 min. To visualize the nucleus, cells were incubated with DRAQ5 (1:300 in PBS) (Biostatus Limited) for 10 min or DAPI (Invitrogen) for 1 min. Samples were mounted using MOWIOL mounting medium (Calbiochem).

Antibodies and dilutions used are as follows: 2E6 (kindly provided by M.M.Mota, 1:2500), anti-UIS4 (kindly provided by M.M.Mota, 1:500), anti-GFP (Invitrogen, 1:100), anti-EEA1 (Sigma, 1:500), anti-TfR (Zymed, 1:100), anti-LAMP1 (Hybridoma Bank, University of Iowa, 1:300) and anti-CD63 (MBL International, 1:500). Secondary antibodies goat anti-mouse Alexa and goat anti-rabbit Alexa (Invitrogen) were all used at 1:400. The 2 μm latex beads were from Sigma.

Virus production and cell transduction

cDNA of mouse Rab5a and Rab7a, including the UTR, were amplified and cloned into the modified mammalian vector pEGFP as described by Lopes et al. (21). The resulting plasmids were used to generate pAd adenoviral vector and viral particles as described previously (22). Adequate virus titers to give GFP expression in 80–90% of cells were used and added to cells for at least 20 h of plasmid expression.

Live cell imaging

Hepa1-6 cells (4×10^4) were seeded on glass bottom culture dishes (MatTek Corporation) and infected with 5×10^4 GFP-*P. berghei* sporozoites. Samples were visualized using an inverted Leica SP5 confocal microscope with a resonance scanner and fitted with a temperature and CO_2 control chamber. LysoTracker®Red (Invitrogen) was added to cells according to the manufacturer's protocol. To visualize acidic vesicles, pHrodo™Dextran (Invitrogen) was added to cells (70 μg/ml) for 12–16 h, then washed with growth medium and incubated for a further 2–3 h (chase) to accumulate the dye in the late lysosomal pathway. Acquisition settings were not changed between different samples.

The 2 μm latex beads were incubated with cells for 3 h, washed with growth medium before the addition of LysoTracker®Red and visualization. For pHrodo™dextran experiments, cells were incubated with pHrodo™dextran for 16 h, washed and beads were added during the 3-h chase.

Drug concentrations

Ammonium chloride (NH_4Cl) (Sigma) was incubated with cells at a final concentration of 25 mM in growth medium. Concanamycin A (Sigma) was used at 0.1 nM in growth medium.

Image analysis

Infection rate, unless otherwise stated, reflects the total number of parasites in one coverslip. Nuclei were also counted to ensure similar cell confluency in all samples. To measure schizont size, between 20 and 30 images of liver schizonts, for each condition, were acquired using an SP5 Leica confocal microscope. The circumference of each schizont was drawn manually, and schizont area (in μm^2) was calculated automatically using ImageJ (NIH).

To quantify vesicle aggregation around *P. berhgei* parasites at least 50 parasite vacuoles, for each time point, were scored for either 'positive' or 'negative' aggregation. Radial intensity profiles (ImageJ) were analyzed for each parasite and aggregation was only scored 'positive' when a peak of fluorescence intensity (at least two times that of the cell cytoplasmic levels) was found within 3 μm of the parasite edge. Results are shown as a percentage of total parasites counted for each time point.

EM sample preparation

Hepa1-6 cells were infected with GFP-*P. berghei* parasites and at 3–5 hpi were cell-sorted to enrich for infected cells using a FACSAria cell sorter (BD). Sorted cells were seeded on Thermanox (Nunc) coverslips and further incubated in growth medium until ready to fix at the indicated time-points. Cells were fixed in 2% PFA (Sigma) and 2% glutaraldehyde (Electron Microscopy Sciences) in 0.1 M sodium cacodylate buffer for 30 min. After washing in 0.1 M sodium cacodylate buffer, cells were post-fixed in 1.5% potassium ferricyanide (Sigma) and 1% Osmium tetroxide (Sigma) for 1 h on ice. Cells were subsequently incubated in 1% tannic acid in 0.05 M sodium cacodylate for 45 min and dehydrated in ethanol (70%, 90% and absolute). Coverslips were then transferred to 1:1 propylene oxide: Epon for 1 h, followed by two changes and embedding in Epon.

Ultra-thin sections (70 nm) were stained with lead citrate before examination on a JEOL 1010 TEM (Welwyn Garden City, UK). Images were taken with a Gatan OriusSC100B charge-coupled device camera and analyzed with Gatan Digital Micrograph and ImageJ (NIH).

Fluid phase HRP loading and DAB reaction

To load vesicles from the endocytic pathway with HRP (Sigma), cells were incubated for 12–16 h with HRP (5 mg/mL, Sigma) in growth medium, washed and further incubated for 2–3 h before fixation with 2% PFA and 2% glutaraldehyde in 0.1 M sodium cacodylate buffer for 30 min. Cells were then washed in 0.1 M Tris Buffer (pH 7.6) and incubated with 0.1 M Tris buffer containing 100 μg/mL diaminobenzidine (DAB) (Sigma) and 0.015% H_2O_2 (Sigma) at room temperature in the dark for 30 min. Cells were washed with 0.1 M Tris buffer, osmicated, dehydrated and embedded as described above.

BSA-gold production and uptake

A 10 nm BSA-gold was produced following the protocol described by Slot and Geuze (23).

BSA-gold was added to the culture medium and allowed to enter cells for 16 h before fixation and TEM sample preparation as described above.

Statistical analysis

Statistical analysis was performed using Prism software (GraphPad Software Inc.) using an unpaired Student *t* test; $p < 0.05$ was considered statistically significant. Unless otherwise stated, graphs show mean of triplicate samples with ±SEM.

Acknowledgments

This work was supported by Fundação para a Ciência e Tecnologia (FCT), Portugal. The authors would like to thank Dr. Maria M. Mota and all the members of her laboratory for mosquito rearing, antibodies and very helpful discussions during the course of this work. We also wish to thank Ligia A. Gonçalves for help with primary hepatocyte isolation and the IGC imaging unit, specially Dr. Nuno Moreno, for help with microscopy and image

analysis. We also want to thank Dr. Maria M. Mota for critically reading the manuscript. M. L. S. was funded by FCT grant SFRH/BD/27705/2006, C. T. M. was funded by FCT grant SFRH/BD/45458/2008, L. C. S. was funded by FCT grant SFRH/BPD/65764/2009. M. C. S. is the recipient of a Gulbenkian Mid-Career Fellowship. The authors declare no conflict of interests.

Supporting Information

Additional Supporting Information may be found in the online version of this article:

Figure S1: *Plasmodium berghei* parasites are surrounded by GFP-Rab7a but not transferrin receptor in Hepa1-6 cells, and are surrounded by LAMP1-positive vesicles in isolated mouse primary hepatocytes. A) Hepa1-6 cells where infected with GFP-*P. berghei* sporozoites and infection was stopped at various times post-infection. Cells were stained with anti-TfR (red) and anti-GFP (green) antibodies. Same images as in Figure 1 with separate color channels shown here for clarity. B) Hepa1-6 cells were transduced with GFP-Rab7a (red) prior to infection with *P. berghei* sporozoites, fixed at the time-points indicated and subsequently stained with 2E6 (green). Same images as in Figure 2 with separate color channels shown here for clarity. C) Isolated primary mouse hepatocytes were infected with GFP-*P. berghei* sporozoites and fixed at the time-points indicated. Cells were stained using anti-LAMP1 antibody (red) and anti-GFP (green). Hpi, hours post-infection. Scale bars: 10 μm.

Figure S2: Hepa1-6 cells internalize latex beads and fuse with LysoTracker®Red and pHrodo™dextran-positive. A) Hepa1-6 cells were fed latex beads (bright field) for 3 h before the addition of LysoTracker®Red and visualization. Scale bar: 5 μm. B) Hepa1-6 cells were incubated with pHrodo™dextran for 16 h, washed and latex beads were added during the 3 h chase. Scale bar: 5 μm.

Movie S1: Movement of LysoTracker®Red acidic vesicles in the vicinity of *Plasmodium berghei* liver parasites. Hepa1-6 cells were infected with GFP-*P. berghei* sporozoites and infection was allowed to proceed. Prior to visualization LysoTracker®Red was added to cells. Time-lapse images showing GFP-*P. berghei* parasite at 16 h post-infection in green and LysoTracker®Red stained vesicles shown in red. Representative images are shown in Figure 5. Scale bar: 5 μm.

Please note: Wiley-Blackwell are not responsible for the content or functionality of any supporting materials supplied by the authors. Any queries (other than missing material) should be directed to the corresponding author for the article.

References

1. Mota MM, Pradel G, Vanderberg JP, Hafalla JC, Frevert U, Nussenzweig RS, Nussenzweig V, Rodríguez A. Migration of Plasmodium sporozoites through cells before infection. Science 2001;291:141–144.
2. Albuquerque SS, Carret C, Grosso AR, Tarun AS, Peng X, Kappe SHI, Prudêncio M, Mota MM. Host cell transcriptional profiling during malaria liver stage infection reveals a coordinated and sequential set of biological events. BMC Genomics 2009;10:270.
3. Stanway RR, Mueller N, Zobiak B, Graewe S, Froehlke U, Zessin PJM, Aepfelbacher M, Heussler VT. Organelle segregation into Plasmodium liver stage merozoites. Cell Microbiol 2011;13:1768–1782.
4. Sturm A, Graewe S, Franke-Fayard B, Retzlaff S, Bolte S, Roppenser B, Aepfelbacher M, Janse C, Heussler V. Alteration of the parasite plasma membrane and the parasitophorous vacuole membrane during exo-erythrocytic development of malaria parasites. Protist 2009;160:51–63.
5. Sinnis P, Sim BK. Cell invasion by the vertebrate stages of Plasmodium. Trends Microbiol 1997;5:52–58.
6. Méresse S, Steele-Mortimer O, Moreno E, Desjardins M, Finlay B, Gorvel JP. Controlling the maturation of pathogen-containing vacuoles: a matter of life and death. Nat Cell Biol 1999;1:E183–E188.
7. Vergne I, Chua J, Lee H-H, Lucas M, Belisle J, Deretic V. Mechanism of phagolysosome biogenesis block by viable *Mycobacterium tuberculosis*. Proc Natl Acad Sci USA 2005;102:4033–4038.
8. Isberg RR, O'Connor TJ, Heidtman M. The *Legionella pneumophila* replication vacuole: making a cosy niche inside host cells. Nat Rev Microbiol 2009;7:13–24.
9. Bano N, Romano JD, Jayabalasingham B, Coppens I. Cellular interactions of Plasmodium liver stage with its host mammalian cell. Int J Parasitol 2007;37:1329–1341.
10. Jayabalasingham B, Bano N, Coppens I. Metamorphosis of the malaria parasite in the liver is associated with organelle clearance. Cell Res 2010;20:1043–1059.
11. Deschermeier C, Hecht L-S, Bach F, Rützel K, Stanway RR, Nagel A, Seeber F, Heussler VT. Mitochondrial lipoic acid scavenging is essential for *Plasmodium berghei* liver stage development. Cell Microbiol [Internet] 2011 [cited 2012 Jan 19]; Available from http://www.ncbi.nlm.nih.gov/pubmed/22128915.
12. Flannagan RS, Cosío G, Grinstein S. Antimicrobial mechanisms of phagocytes and bacterial evasion strategies. Nat Rev Microbiol 2009;7:355–366.
13. van Deurs B, Holm PK, Sandvig K. Inhibition of the vacuolar H(+)-ATPase with bafilomycin reduces delivery of internalized molecules from mature multivesicular endosomes to lysosomes in HEp-2 cells. Eur J Cell Biol 1996;69:343–350.
14. Gordon AH, Hart PD, Young MR. Ammonia inhibits phagosome-lysosome fusion in macrophages. Nature 1980;286:79–80.
15. Dröse S, Altendorf K. Bafilomycins and concanamycins as inhibitors of V-ATPases and P-ATPases. J Exp Biol 1997;200:1–8.
16. Sobota JA, Bäck N, Eipper BA, Mains RE. Inhibitors of the V0 subunit of the vacuolar H+−ATPase prevent segregation of lysosomal- and secretory-pathway proteins. J Cell Sci 2009;122:3542–3553.
17. Yates RM, Hermetter A, Russell DG. The kinetics of phagosome maturation as a function of phagosome/lysosome fusion and acquisition of hydrolytic activity. Traffic 2005;6:413–420.
18. Coppens I, Dunn JD, Romano JD, Pypaert M, Zhang H, Boothroyd JC, Joiner KA. *Toxoplasma gondii* sequesters lysosomes from mammalian hosts in the vacuolar space. Cell 2006;125:261–274.
19. Gonçalves LA, Vigário AM, Penha-Gonçalves C. Improved isolation of murine hepatocytes for in vitro malaria liver stage studies. Malar J 2007;6:169.
20. Franke-Fayard B, Trueman H, Ramesar J, Mendoza J, van der Keur M, van der Linden R, Sinden RE, Waters AP, Janse CJ. A *Plasmodium berghei* reference line that constitutively expresses GFP at a high level throughout the complete life cycle. Mol Biochem Parasitol 2004;137:23–33.
21. Lopes VS, Ramalho JS, Owen DM, Karl MO, Strauss O, Futter CE, Seabra MC. The ternary Rab27a-Myrip-Myosin VIIa complex regulates melanosome motility in the retinal pigment epithelium. Traffic 2007;8:486–499.
22. Hume AN, Tarafder AK, Ramalho JS, Sviderskaya EV, Seabra MC. A coiled-coil domain of melanophilin is essential for Myosin Va recruitment and melanosome transport in melanocytes. Mol Biol Cell 2006;17:4720–4735.
23. Slot JW, Geuze HJ. A new method of preparing gold probes for multiple-labeling cytochemistry. Eur J Cell Biol 1985;38:87–93.